Geophysical Research Letters

RESEARCH LETTER
10.1029/2020GL087212

Eurasian Cooling Linked to the Vertical Distribution of Arctic Warming

Shengping He[1], Xinping Xu[2], Tore Furevik[1], and Yongqi Gao[3,4]

[1]Geophysical Institute, University of Bergen and Bjerknes Centre for Climate Research, Bergen, Norway, [2]Collaborative Innovation Center on Forecast and Evaluation of Meteorological Disasters/Key Laboratory of Meteorological Disaster, Ministry of Education, Nanjing University of Information Science and Technology, Nanjing, China, [3]Nansen Environmental and Remote Sensing Center and Bjerknes Centre for Climate Research, Bergen, Norway, [4]Nansen-Zhu International Research Center, Institute of Atmospheric Physics, Chinese Academy of Sciences, Beijing, China

Key Points:
- Winter Arctic warming simulated by climate models can be shallowly at near-surface or deeply extend into the upper troposphere
- Deep Arctic warming is linked to more moisture and heat into the Arctic induced by a poleward shift of North Atlantic storm track
- Climate models are likely to replicate warmer Arctic-colder Eurasia pattern when they simulate a deep rather than a shallow Arctic warming

Supporting Information:
- Supporting Information S1

Correspondence to:
S. He,
shengping.he@uib.no

Citation:
He, S., Xu, X., Furevik, T., & Gao, Y. (2020). Eurasian cooling linked to the vertical distribution of Arctic warming. *Geophysical Research Letters*, *47*, e2020GL087212. https://doi.org/10.1029/2020GL087212

Received 23 JAN 2020
Accepted 21 APR 2020
Accepted article online 23 APR 2020

Abstract Observations show that deep Arctic winter warming, extending from surface to mid-troposphere, has concurred with below-average temperature over central Eurasia. Modeling studies focusing on the response to Arctic sea ice loss have shown Arctic surface warming but no consistent atmospheric changes at midlatitude. Using a large number of simulations from coupled and uncoupled climate models, we show that Eurasian below-average temperatures are more frequent in winters with deep warming compared to shallow, near-surface warming over the Barents-Kara Seas. Dramatic weakening of the midlatitude jet stream and increase in Ural blocking frequency are more likely to occur in winters with deep Arctic warming. Deep warming is independent of sea ice forcing but follows increased poleward atmospheric energy and moisture advection from the North Atlantic to the Arctic, indicating that internal natural variability and not sea ice is the main driving forcing for deep Arctic warming-cold Eurasia pattern in historical simulations.

Plain Language Summary Observations show that the amplitude of Earth surface warming since the mid-twentieth century over the Arctic is more than twice as large as that of the global average. At the same time Eurasia has seen many extreme cold winters. Previous modeling studies have reached no consensus on whether the Arctic warming is influencing the Eurasian winter climate or not. Here we demonstrate that the simulated Arctic warming events are very different in their vertical extension and that Eurasian cold winters are more frequent when there is an Arctic warming aloft. This is caused by enhanced heat and moisture transport from the North Atlantic.

1. Introduction

Observations show that the amplitude of warming since the mid-twentieth century over the Arctic is more than twice as large as the global average (Blunden & Arndt, 2012; Huang et al., 2017) and that the Arctic sea ice has dramatically declined since the satellite era (Stroeve & Notz, 2018). It has been suggested that less sea ice and a warmer Arctic in winter induce anomalous atmospheric circulation and climate at midlatitude through modulation of the tropospheric jet streams (Francis & Vavrus, 2012; Haarsma et al., 2013; Peings & Magnusdottir, 2014), the Siberian high (Cohen et al., 2012; Nakamura et al., 2015), the stratospheric polar vortex (Kim et al., 2014; Kretschmer et al., 2016; Zhang et al., 2018), the Arctic Oscillation (King et al., 2016; Zhang et al., 2016), or Eurasian land feedback (Nakamura et al., 2019). However, no consensus has been reached on the role of the Arctic warming in the Eurasian cooling or on the various mechanisms involved.

Despite great effort from the scientific community to understand the potential influence of the Arctic on climate at midlatitude, conclusions seem to have diverged instead of converged in recent years (Barnes & Screen, 2015; Cohen et al., 2020; Francis, 2017; Meleshko et al., 2016). Many recent studies claim explicitly that there is no robust response of Eurasian winter climate to Arctic sea ice loss, showing a lack of cold anomalies (Blackport et al., 2019; McCusker et al., 2016), a non-robust increase in extreme weather events (Chen et al., 2016; Screen, 2017), or an absence of cooling trend (Collow et al., 2018; Ogawa et al., 2018). Some studies suggest that the Arctic-Eurasian climate linkage might be induced simultaneously by internal variability and tropical forcing (Matsumura & Kosaka, 2019; Warner et al., 2020). The discrepancies in findings necessitate a robust model-to-model and model-to-observation comparison and an in-depth

investigation into the proposed mechanisms and pathways for the Arctic-to-midlatitude linkages (Cohen et al., 2014).

It is noteworthy that while the observed Arctic warming extends deep into the upper troposphere (Screen et al., 2012; Screen & Simmonds, 2010), the simulated Arctic warming of multimodel ensemble mean in coupled climate models has smaller magnitude and shallower vertical extent than observations, with relatively deeper vertical extent. In uncoupled climate models the signal is even weaker (Cohen et al., 2020; Deser et al., 2015). There are only a few individual ensemble members that closely match the vertical distribution of observed temperature trends, indicating the contribution of internal variability to the simulated and observed divergences (Ogawa et al., 2018). Nevertheless, previous studies have suggested that an Arctic near-surface warming is not sufficient to change the meridional temperature gradient or the zonal-mean jet stream (Coumou et al., 2018) and that a midlatitude response can only be excited if the Arctic winter warming signal extends to the model's tropopause (Sellevold et al., 2016). Observational analysis has already indicated that severe winter weather became more frequent in the eastern United States when the Arctic warming extends into the upper troposphere and lower stratosphere (Cohen et al., 2018). We, therefore, hypothesize that the responses in Eurasian winter temperatures to shallow Arctic warming (i.e., surface and near-surface warming) versus deep Arctic warming (i.e., tropospheric warming) in climate models are very different.

2. Data and Methods

2.1. Climate Models Simulations

Historical monthly simulations are obtained from 36 fully coupled general circulation models (CGCMs) in the Coupled Model Intercomparison Project Phase 5 (CMIP5) (Table S1) during 1900–2005. The daily analyses are based on a subset of 13 CMIP5 models that provide consistently the daily atmospheric variables for 1950–2005 (Table S1). Only the first ensemble member (r1i1p1) of each model was used. Forty ensemble members of simulations from the Community Earth System Model Large Ensemble (CESM-LE) are employed (1920–2005); each ensemble member is subject to the same radiative forcing scenario but begins from a slightly different initial atmospheric state (Kay et al., 2015). One hundred thirty ensemble members of hindcast simulations for 1982–2014 were performed by six atmospheric general circulation models (atmosphere only) under the NordForsk funded GREENICE project (https://greenice.b.uib.no/), and each was forced by prescribed climatological sea surface temperatures and daily varying sea ice concentrations during 1982–2014. Sea ice thickness was not prescribed, which might have influenced the atmospheric response to sea ice loss (Labe et al., 2018). All experiments are forced with the CMIP5 historical forcing for 1982–2005 and Representative Concentration Pathway 8.5 for 2006–2014 (Ogawa et al., 2018).

2.2. Definitions of Shallow Arctic Warming and Deep Warming Cases

The Arctic surface temperature index (ATI_2m) is defined as the area-averaged surface air temperature (SAT) over the Barents-Kara Seas (BKS; 70°–80°N, 30°–70°E) (Kug et al., 2015), and the Arctic tropospheric temperature index (ATI_500) is defined as the area-averaged air temperature at 500 hPa over the same region. Both indices are detrended and normalized. For the monthly data from CMIP5, the deep Arctic warming winters (60% of total warming winters) are identified when both ATI_2m and ATI_500 exceed 0.5 standard deviation (STD), while the shallow Arctic warming winters (40% of total warming winters) are identified when ATI_2m is above 0.5 STD and ATI_500 is below 0.5 STD. The same method is applied to GREENICE and CESM-LE simulations to choose shallow Arctic warming and deep warming winters. A synoptic shallow Arctic warming event (37% of total warming cases) is defined to take place if (i) the daily normalized ATI_2m reaches its relative maximum on 1 day (referred as 0 day), and the day prior to and after this day have a value of ATI_2m greater than or equal to +1 STD, and (ii) the normalized ATI_500 are less than +1 STD during the same days. A synoptic deep Arctic warming event (63% of total warming cases) is defined to take place if the daily normalized ATI_2m satisfies the above condition (i) and one or more of these 3 days have a value of ATI_500 greater than or equal to +1 STD. In all synoptic-scale analyses, the 0 day will be referred to as the day for the peaking of Arctic warming case. All data were linearly detrended and daily data were further applied 10 days low pass filter. Winter mean is defined as the average of December and the following January and February.

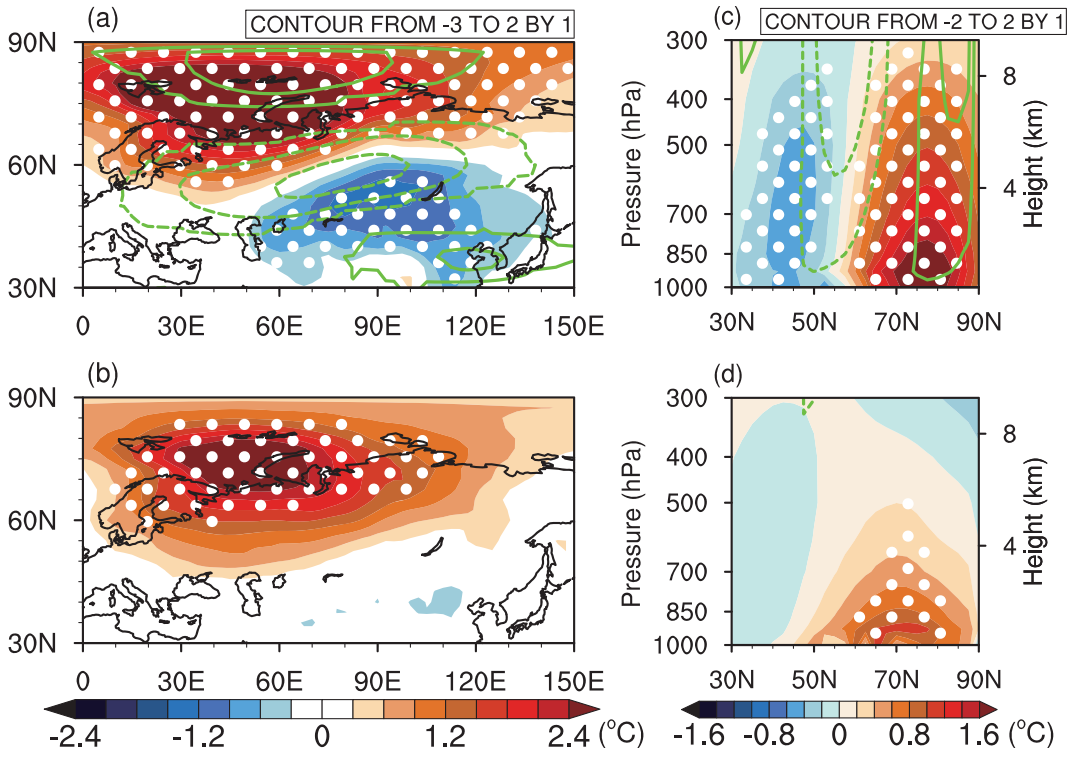

Figure 1. (a, b) Composites of winter SAT anomalies (shading; °C) and 300 hPa zonal wind anomalies (contours; with the interval of 1) in winters with (a) deep Arctic warming and (b) shallow Arctic warming derived from ensemble mean of 36 CGCMs in CMIP5 historical simulations during 1900–2004. (c, d) same as (a, b), but for composites of winter zonal-mean temperature and zonal wind anomalies along 0°–150°E. Temperature/zonal wind anomalies where more than 90% of the models agree on the sign of the ensemble mean are shown as stippling/green contours.

3. Results

3.1. Shallow Versus Deep Arctic Winter Warming

We first compare the winter atmospheric anomalies between shallow and deep Arctic warming winters from CMIP5 outputs. In winters with a deep Arctic warming, there is a strong surface warming in the BKS that exceeds 2.4 °C (Figure 1a, colors). At the same time, there are lower than normal temperatures over central Eurasia. Both the warm and cold signals extend into the upper troposphere (Figure 1c, colors). In contrast, winters with shallow Arctic warming have the surface warming signal over the BKS but lack the Eurasian cold signal (Figure 1b). Furthermore, the warming signal is, by the definition of our composites, confined to the lower part of the troposphere (Figure 1d). The upper tropospheric zonal wind at midlatitude (50°–65°N, 40°–110°E) associated with deep Arctic warming shows pronounced negative anomalies (Figure 1a, contours). For the shallow warming winters, there is no dramatic reduction of the midlatitude jet stream over Eurasia (no contours in Figure 1b). To further elucidate the dominant climate feature in winters with deep Arctic warming, we show that winters with warming aloft but without warming at the surface also have significant colder anomalies over central Eurasia as well as the reduction in the midlatitude jet stream (Figure S1). This further implies the stronger connection of Arctic warming aloft with the midlatitude climate compared to shallow surface warming. Note that the results are similar if the domain of ATI_2m is expanded to the entire Arctic (north of 67°N), reflecting that the Arctic warming hotspot area is indeed the BKS (Lind et al., 2018).

In winters with deep Arctic warming, the blocking events (method from Luo et al., 2015) increase by up to 6% relative to the climatology in the ensemble mean over North Europe, especially around the Ural Mountains (Figure 2a, shading). Such a feature is consistent across more than 90% models (Figure 2a, stippling). Meanwhile, there is an increase in the number of extreme cold days (definition from Kolstad et al., 2010) at Eurasian midlatitude (Figure 2c) due to the southward cold air advection induced by the

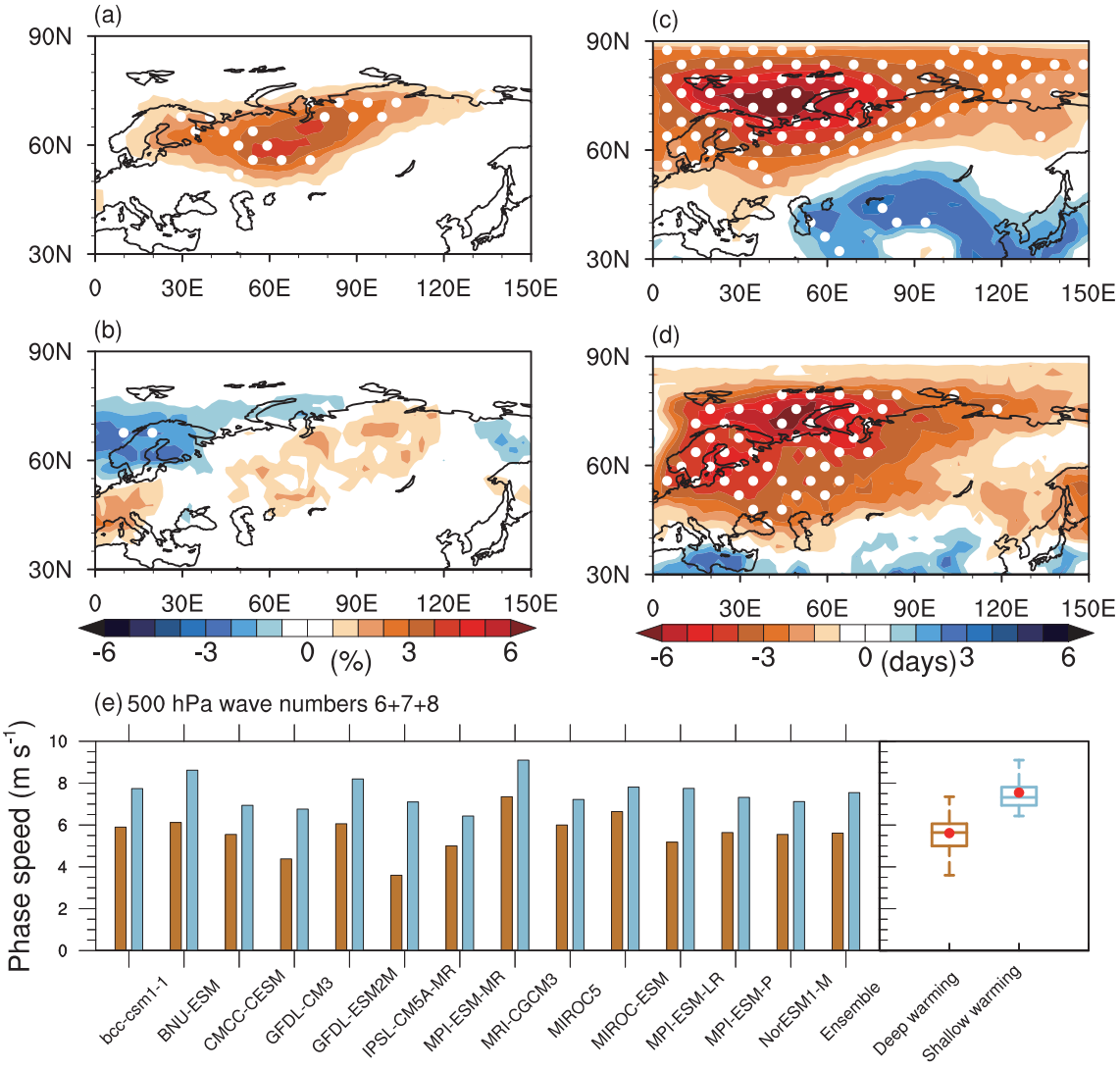

Figure 2. Composites of (a, b) winter blocking frequency anomalies (%) and (c, d) number of winter extreme cold days anomalies (days) in winters with (a, c) deep Arctic warming and (b, d) shallow Arctic warming derived from ensemble-mean of 13 CGCMs in CMIP5 historical simulations during 1950–2004. Regions, where more than 90% of the models agree with the sign of the ensemble mean, are marked with white stippling. (e) The phase speed at 500 hPa averaged over 50°–65°N, 40°–110°E for the wavenumbers 6 to 8 on the peaking of Arctic warming day (see method); red and blue bars indicate the deep Arctic warming cases and shallow Arctic warming cases, respectively. Box plots for the ensemble mean are shown to the right.

Ural blocking (UB) (Blackport et al., 2019; Ye et al., 2018). In contrast, when the Arctic warming is confined to near surface, the increase in blocking frequency over the Ural Mountains is very weak (<3%, Figure 2b, shading), and the model spread is large (Figure 2b, less stippling). Also, the frequency of extreme cold days over Eurasia does not show a significant increase (Figure 2d). The more increasing of UB frequency in winters with deep Arctic warming is consistent with a relatively weak Rossby wave phase speed (method from Coumou et al., 2014) (Figure 2e). Previous studies have also linked the increase in blocking events and extreme weather at midlatitude to the inflated Arctic atmospheric thickness (Francis & Vavrus, 2012; Overland & Wang, 2010), anomalous anticyclone over the Ural Mountain (Peings, 2019) as well as the anomalous ascending motions in the BKS (Xu et al., 2019). Here, we demonstrate that such changes of large-scale atmospheric circulation occur mainly in deep Arctic warming winters. For example, there are anomalous ascending motions over the BKS associated with deep Arctic warming (Figure S2a), which bend eastward and southward to midlatitude where the flow turns into anomalous easterlies (Figure S2b). This large-scale atmospheric circulation exhibits an anomalous anticyclone with a

barotropic structure located in North Eurasia (Figure S2b), while it is much weaker in shallow Arctic warming winters (not shown).

3.2. Deep Arctic Warming and Atmospheric Internal Variability

The above analyses have shown that the atmospheric anomalies associated with deep Arctic warming winters are more dominant than that associated with shallow Arctic warming winters. The differences can partly explain why most climate models replicate the Arctic near-surface warming but do not reproduce the colder winters over central Eurasia (McCusker et al., 2016). It suggests a way to reconcile the differences between the observed and simulated Arctic warming and further to improve our understanding of the Arctic-midlatitude climate linkage. Since the UB and the Arctic warming aloft are internal variability of the atmosphere, the differences in the representation of Arctic-midlatitude climate linkage could be due to natural variability. To further explore this, we first use outputs from atmosphere-only GREENICE simulations. Figures 3a–3f show the winter SAT and sea level pressure (SLP) anomalies in winters with deep Arctic warming in the six models. Here we see significant warming over the Arctic and significant colder anomalies over central Eurasia in all the six models. Such a feature is associated with significant intensification of pressure throughout the Ural Mountain (around 60°E), indicating the abovementioned close relationship between the deep Arctic warming and the UB. By contrast, the winters with shallow Arctic warming did not show significant cooling over central Eurasia (Figures 3h–3m). This feature is robust in all six models, which also show consistently that the shallow Arctic warming winters are not associated with significant positive pressure anomaly throughout the Ural Mountain (around 60°E). Additionally, regression of winter SAT in the six climate models from GREENICE onto the BKS sea ice prescribed in these experiments only shows significant warmer conditions at the near surface over the BKS without significant colder conditions over Eurasia (Figure S3). Given that all ensemble members of each individual model had the same boundary and radiative conditions, and only the atmospheric initial conditions were perturbed, the results derived from GREENICE suggest that the deep Arctic warming-cold Eurasia pattern is not forced by Arctic sea ice loss but is related to the atmospheric internal variability.

To further elucidate the above conclusion, we choose winters with respectively shallow and deep Arctic warming from a 40-ensemble-members simulation with historical forcing in CESM-LE (Kay et al., 2015). The SAT anomalies from the winters with deep Arctic warming display significant positive anomalies over the Arctic and significant negative anomalies over central Eurasia, accompanied with significant positive pressure anomalies over the Ural Mountain (Figure 3g). Unlike the situations of deep Arctic warming, shallow Arctic warming winters are associated with positive SAT anomaly over central Eurasia and negative pressure anomaly over the Ural Mountain (Figure 3n). Again, it should be noted that all ensemble members have the same boundary conditions and that they only differ in their initial air temperature (Kay et al., 2015). The analyses on the CESM-LE simulations confirm the close link between deep Arctic warming and the colder winters over central Eurasia and the intensified UB.

3.3. Lead-Lag Relationship Inferred From Intraseasonal Scale Analyses

The above analyses based on monthly mean outputs from climate models show that compared to the situations associated with shallow Arctic warming, the deep Arctic warming is associated with more frequent UB and stronger anomalous anticyclone over northern Eurasia. This does not prove causality. On the one hand, deep Arctic warming can potentially alter the large-scale atmospheric circulation at Eurasian midlatitude (Cohen et al., 2014; Francis & Vavrus, 2012; Kug et al., 2015; Overland & Wang, 2010; Vavrus, 2018). On the other hand, anomalous atmospheric circulation outside the Arctic may conversely contribute to the Arctic warming through inducing adiabatic warming (Ding et al., 2014; Lee et al., 2011) or increasing warm and moist air into Arctic (Lee et al., 2017; Wernli & Papritz, 2018).

The causality might be inferred from intraseasonal scale analyses showing the lead-lag relationship. On synoptic scale, the peaking of middle tropospheric (500 hPa) air temperature over the BKS leads the peaking of SAT by 1 day (−1 day; first curves in Figure 4a), indicating that the Arctic warming aloft is not induced by surface warming. Interestingly, central Eurasia reaches the lowest temperature (+2 days in the fourth curves of Figure 4a) after the peaking of Arctic warming aloft. The maximum decrease in temperature in central Eurasia associated with the deep Arctic warming case ranges from −3.4 to −1.0°C among the multimodel ensembles and is followed by colder anomalies for about 10 days. Both the

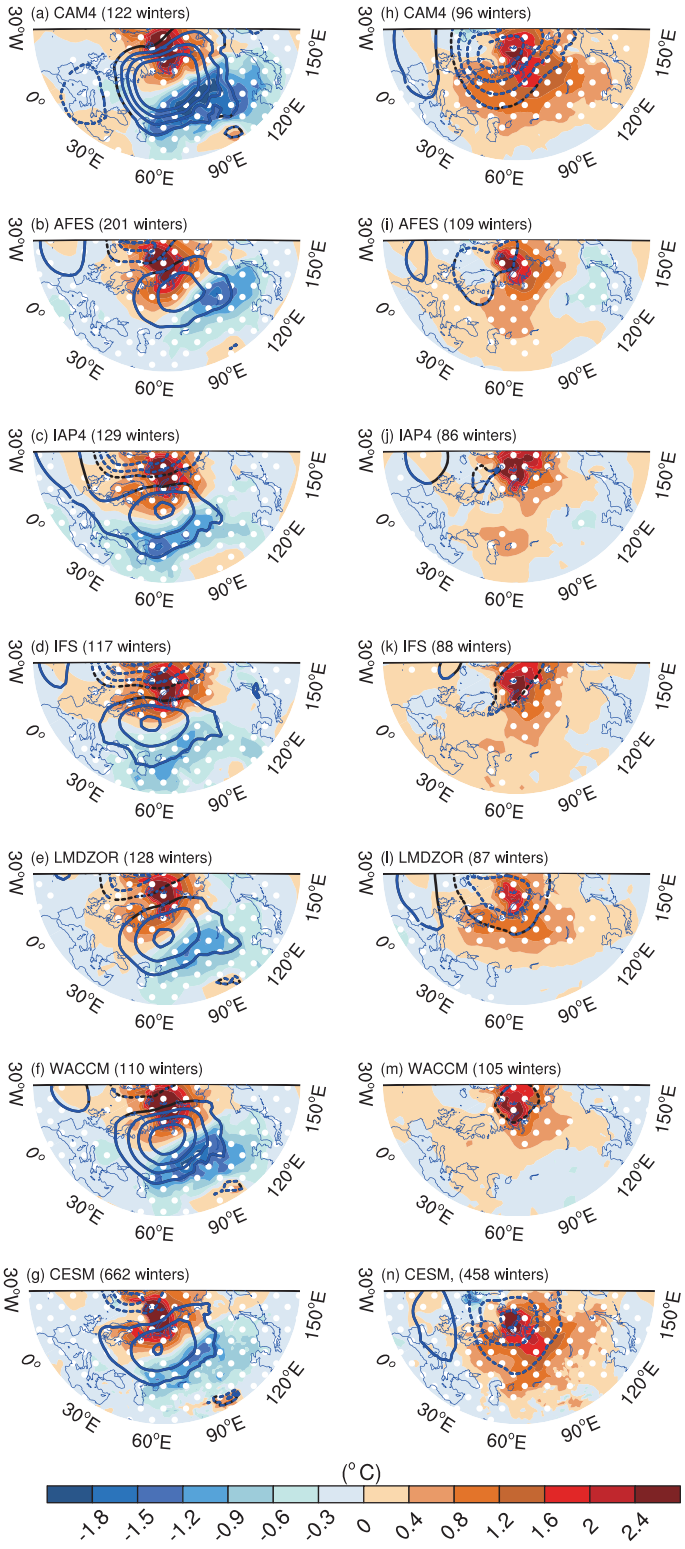

Figure 3. (a–f) Winter SAT (shading, °C) and SLP (contours, hPa; interval is one and 0-contour is ignored) anomaly (relative to the climatology during 1982–2013 winter for all ensemble members) in GREENICE ensemble members which have deep Arctic warming; the number of such winters in each model is given. Stippling shading/blue contours indicate the SAT/SLP anomalies statistically significant at 90% confidence level. (h–m) as (a–f), but for the GREENICE ensemble members which have shallow Arctic warming. (g) and (n) as (a) and (h), respectively, but for the historical simulations (winters for 1920–2004) from CESM-LE.

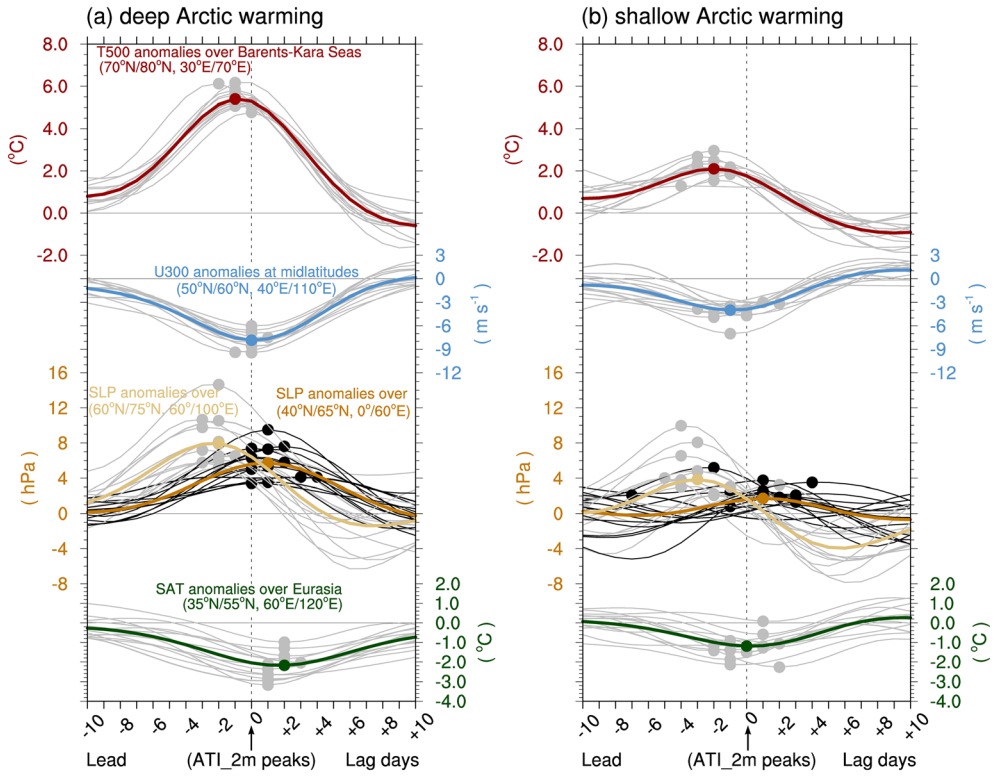

Figure 4. (a) Anomalies associated with deep Arctic warming cases, from top to bottom: area-averaged anomalies of 500-hPa air temperature (T500) over the BKS, 300-hPa zonal wind (U300) anomalies at midlatitude, SLP anomalies in the west (dark color curves) and east (light color curves) of Ural sector, and SAT anomalies over central Eurasia; thin (thick) lines indicate results of individual model (multi-model ensemble mean), and 0 at *x*-axis denotes ATI_2m reaches its relative maximum (see method); negative/positive values at *x*-axis indicate the days before/after the peaking Arctic warming. The dots indicate the days when the time series reach maximum/minimum values. (b) same as (a), but for the shallow Arctic warming cases.

maximum amplitude and the duration are about twice as large as those that associated with the shallow Arctic warming (the fourth curves in Figure 4b). The longer-lasting and larger magnitude of the central Eurasian winter cold anomalies could be related to a stronger weakening of westerly winds at midlatitude (second curves in Figures 4a and S4) due to deep warming over the Arctic which can lead to more persistence in weather patterns (Cohen et al., 2014; Francis & Vavrus, 2012) and in the UB (Luo et al., 2016). Though the influence of the UB on Arctic warming has also been suggested by some studies (Luo et al., 2016), we note that there are many different definitions of the Ural sector, which in some cases extend west to 10°W (Peings, 2019) or east to 100°E (Tyrlis et al., 2019). We do see dominant high-pressure anomalies over the Ural sector before and after the peaking of Arctic warming (in both shallow and deep warming cases) (Figure S5). In the deep Arctic warming cases, however, the positive SLP anomalies extend more westward, with distinctive evolution in the east and west of Ural sector. For example, the SLP over (60°–75°N, 60°–100°E) (Tyrlis et al., 2019) reaches a maximum before the peaking of deep Arctic warming (the third curves in light color of Figure 4a), which is consequently followed by more intensification of the pressure in the west of Ural sector (the third curves in dark color of Figure 4a). This indicates an interaction between deep Arctic warming and the UB. The extreme westward extent of the UB is likely triggered by an intensified quasi-stationary Rossby wave (Honda et al., 2009). Such a mechanism is visible by inspecting Figures S5 and S6. Prior to a deep Arctic warming (especially from −3 days to −1 day), Rossby wave fluxes (vectors; method from Takaya & Nakamura, 2001) propagate from the BKS to North Eurasia where the SLP strengthens and extends westwards concurrently. After the peaking of deep Arctic warming (0 day), the southwards propagating Rossby wave fluxes persist about 3 days during which the pressure in the west (40°–65°N, 0°–60°E) of Ural sector

continues to strengthen (from +1 day to +3 days; see yellow color in Figures S5 and S6). The above features associated with deep Arctic warming are consistent in multimodel, which is not the case in shallow Arctic warming cases (Figure 4b).

A critical factor for the Arctic-to-midlatitude linkages seems to be the vertical extension of Arctic warming. While Arctic sea ice loss is the main driver for the observed Arctic surface warming (Ogawa et al., 2018) (Figure S3), moist and warm air advection into the Arctic and poleward atmospheric energy transport seems to be keys to the deep Arctic warming (Graversen et al., 2008). On synoptic time scales, maximum poleward water vapor transport and poleward atmospheric energy transport occur 2 to 3 days prior to the peaking of deep Arctic warming (Figures S7b–S7d), showing the importance of natural contributions to deep Arctic warming. For example, from about 7 days ahead of deep Arctic warming, there is a poleward shift of storm tracks from the North Atlantic to the Arctic, and it reaches its strongest intensity in the BKS (Figure S7a) before the peaking of poleward water vapor and atmospheric energy transport. As positive storm track activity anomalies are tied to cyclonic eddy forcing to its north and anticyclonic eddy forcing to its south (Lau, 1988), the strong positive storm track activity over the BKS (Figure S8) suggests that the deep Arctic warming can be driven by the storm tracks from the North Atlantic to the Arctic. It might be related to the contribution of the North Atlantic Oscillation and the Greenland blocking (Figure S5), which, however, needs to be investigated in further studies. Though the lead-lag relationship is robust in multimodel historical simulations and does indicate the interactions between deep Arctic warming and midlatitude atmospheric circulation, the causality needs to be confirmed through atmospheric nudging simulations in future.

4. Conclusions

Our conclusions are based on a large number of numerical simulations from both coupled and uncoupled climate models rather than relying on one model only. Some of the key features and mechanisms associated with deep Arctic warming and shallow Arctic warming are illustrated in Figure S9. For deep Arctic warming (Figure S9a), there is a poleward shift of North Atlantic storm track and a strengthening of the high pressure in the east of Ural sector, both transferring more moisture and energy into the Arctic and causing deep warming. Deep Arctic warming excites a southward propagating Rossby wave train and weakens the midlatitude jet stream, which favors the westward extending of ridge as well as the frequency of the UB. Consequently, below-average temperatures and more extreme cold days occur in winters over central Eurasia. For shallow Arctic warming, there is an anomalous heat transfer from ocean to the atmosphere due to sea ice loss, but negligible responses at midlatitude (Figure S9b).

Previous modeling studies generally show Arctic warming in response to sea ice loss but have discrepancies in their responses at midlatitude. Through separating deep Arctic warming patterns from shallow Arctic warming patterns using both monthly and daily outputs from climate models, we have presented evidence that strongly suggests that climate models are more likely to simulate cold Eurasian winters when there is a deep Arctic winter warming as observed. It suggests that climate models can replicate the warm Arctic-cold Eurasia pattern, but only when the warming signal extends deep into the upper troposphere.

Acknowledgments
Data used in this study are publicly available: (1) CMIP5: http://www.ipcc-data.org/sim/gcm_monthly/AR5/Reference-Archive.html, (2) CESM-LE: http://www.cesm.ucar.edu/projects/community-projects/LENS/, and (3) GREENICE: https://archive.norstore.no/pages/public/datasetDetail.jsf?id=10.11582/2018.00007. This research was supported by a grant from the Norwegian Ministry of Education and Research, the EU H2020 Blue-Action project (Grant 727852), the CONNECTED project supported by UTFORSK Partnership Program (UTF-2016-longterm/10030), and the National Natural Science Foundation of China (Grants 41875118 and 41790472).

References

Barnes, E. A., & Screen, J. A. (2015). The impact of Arctic warming on the midlatitude jet-stream: Can it? Has it? Will it? *Wiley Interdisciplinary Reviews: Climate Change*, *6*, 277–286.

Blackport, R., Screen, J. A., van der Wiel, K., & Bintanja, R. (2019). Minimal influence of reduced Arctic sea ice on coincident cold winters in mid-latitudes. *Nature Climate Change*, *9*(9), 697–704. https://doi.org/10.1038/s41558-019-0551-4

Blunden, J., & Arndt, D. S. (2012). State of the climate in 2011. *Bulletin of the American Meteorological Society*, *93*(7), S1–S264.

Chen, H. W., Zhang, F., & Alley, R. B. (2016). The robustness of midlatitude weather pattern changes due to Arctic sea ice loss. *Journal of Climate*, *29*, 7831–7849.

Cohen, J., Pfeiffer, K., & Francis, J. A. (2018). Warm Arctic episodes linked with increased frequency of extreme winter weather in the United States. *Nature Communications*, *9*(1), 869. https://doi.org/10.1038/s41467-018-02992-9

Cohen, J., Screen, J. A., Furtado, J. C., Barlow, M., Whittleston, D., Coumou, D., et al. (2014). Recent Arctic amplification and extreme mid-latitude weather. *Nature Geoscience*, *7*(9), 627–637. https://doi.org/10.1038/ngeo2234

Cohen, J., Zhang, X., Francis, J., Jung, T., Kwok, R., Overland, J., et al. (2020). Divergent consensuses on Arctic amplification influence on midlatitude severe winter weather. *Nature Climate Change*, *10*(1), 20–29. https://doi.org/10.1038/s41558-019-0662-y

Cohen, J. L., Furtado, J. C., Barlow, M. A., Alexeev, V. A., & Cherry, J. E. (2012). Arctic warming, increasing snow cover and widespread boreal winter cooling. *Environmental Research Letters*, *7*(1), 014007. https://doi.org/10.1088/1748-9326/7/1/014007

Collow, T. W., Wang, W., & Kumar, A. (2018). Simulations of Eurasian winter temperature trends in coupled and uncoupled CFSv2. *Advances in Atmospheric Sciences*, *35*(1), 14–26.

Coumou, D., di Capua, G., Vavrus, S., Wang, L., & Wang, S. (2018). The influence of Arctic amplification on mid-latitude summer circulation. *Nature Communications*, *9*(1), 2959. https://doi.org/10.1038/s41467-018-05256-8

Coumou, D., Petoukhov, V., Rahmstorf, S., Petri, S., & Schellnhuber, H. J. (2014). Quasi-resonant circulation regimes and hemispheric synchronization of extreme weather in boreal summer. *Proceedings of the National Academy of Sciences*, *111*(34), 12331–12336. https://doi.org/10.1073/pnas.1412797111

Deser, C., Tomas, R. A., & Sun, L. (2015). The role of ocean–atmosphere coupling in the zonal-mean atmospheric response to Arctic sea ice loss. *Journal of Climate*, *28*(6), 2168–2186. https://doi.org/10.1175/jcli-d-14-00325.1

Ding, Q., Wallace, J. M., Battisti, D. S., Steig, E. J., Gallant, A. J., Kim, H. J., & Geng, L. (2014). Tropical forcing of the recent rapid Arctic warming in northeastern Canada and Greenland. *Nature*, *509*(7499), 209–212. https://doi.org/10.1038/nature13260

Francis, J. A. (2017). Why are Arctic linkages to extreme weather still up in the air? *Bulletin of the American Meteorological Society*, *98*(12), 2551–2557.

Francis, J. A., & Vavrus, S. (2012). Evidence linking Arctic amplification to extreme weather in mid-latitudes. *Geophysical Research Letters*, *39*, L06801. https://doi.org/10.1029/2012GL051000

Graversen, R. G., Mauritsen, T., Tjernström, M., Källén, E., & Svensson, G. (2008). Vertical structure of recent Arctic warming. *Nature*, *451*(7174), 53–56. https://doi.org/10.1038/nature06502

Haarsma, R. J., Frank, S., & van Oldenborgh, G. J. (2013). Anthropogenic changes of the thermal and zonal flow structure over Western Europe and Eastern North Atlantic in CMIP3 and CMIP5 models. *Climate Dynamics*, *41*(9–10), 2577–2588.

Honda, M., Inoue, J., & Yamane, S. (2009). Influence of low Arctic sea-ice minima on anomalously cold Eurasian winters. *Geophysical Research Letters*, *36*, L08707. https://doi.org/10.1029/2008GL037079

Huang, J., Zhang, X., Zhang, Q., Lin, Y., Hao, M., Luo, Y., et al. (2017). Recently amplified arctic warming has contributed to a continual global warming trend. *Nature Climate Change*, *7*(12), 875–879. https://doi.org/10.1038/s41558-017-0009-5

Kay, J. E., Deser, C., Phillips, A., Mai, A., Hannay, C., Strand, G., et al. (2015). The Community Earth System Model (CESM) large ensemble project: A community resource for studying climate change in the presence of internal climate variability. *Bulletin of the American Meteorological Society*, *96*(8), 1333–1349. https://doi.org/10.1175/Bams-D-13-00255.1

Kim, B. M., Son, S. W., Min, S. K., Jeong, J. H., Kim, S. J., Zhang, X., et al. (2014). Weakening of the stratospheric polar vortex by Arctic sea-ice loss. *Nature Communications*, *5*(1), 4646. https://doi.org/10.1038/ncomms5646

King, M. P., Hell, M., & Keenlyside, N. (2016). Investigation of the atmospheric mechanisms related to the autumn sea ice and winter circulation link in the Northern Hemisphere. *Climate Dynamics*, *46*(3–4), 1185–1195.

Kolstad, E. W., Breiteig, T., & Scaife, A. A. (2010). The association between stratospheric weak polar vortex events and cold air outbreaks in the Northern Hemisphere. *Quarterly Journal of the Royal Meteorological Society*, *136*(649), 886–893. https://doi.org/10.1002/qj.620

Kretschmer, M., Coumou, D., Donges, J. F., & Runge, J. (2016). Using causal effect networks to analyze different Arctic drivers of mid-latitude winter circulation. *Journal of Climate*, *29*, 4069–4081.

Kug, J. S., Jeong, J. H., Jang, Y. S., Kim, B. M., Folland, C. K., Min, S. K., & Son, S. W. (2015). Two distinct influences of Arctic warming on cold winters over North America and East Asia. *Nature Geoscience*, *8*(10), 759–762. https://doi.org/10.1038/ngeo2517

Labe, Z., Peings, Y., & Magnusdottir, G. (2018). Contributions of ice thickness to the atmospheric response from projected Arctic sea ice loss. *Geophysical Research Letters*, *45*, 5635–5642. https://doi.org/10.1029/2018GL078158

Lau, N. C. (1988). Variability of the observed midlatitude storm tracks in relation to low-frequency changes in the circulation pattern. *Journal of the Atmospheric Sciences*, *45*(19), 2718–2743. https://doi.org/10.1175/1520-0469(1988)0452718:Votoms2.0.Co;2

Lee, H. J., Kwon, M. O., Yeh, S. W., Kwon, Y. O., Park, W., Park, J. H., et al. (2017). Impact of poleward moisture transport from the North Pacific on the acceleration of sea ice loss in the Arctic since 2002. *Journal of Climate*, *30*(17), 6757–6769. https://doi.org/10.1175/Jcli-D-16-0461.1

Lee, S., Gong, T., Johnson, N., Feldstein, S. B., & Pollard, D. (2011). On the possible link between tropical convection and the Northern Hemisphere Arctic surface air temperature change between 1958 and 2001. *Journal of Climate*, *24*(16), 4350–4367. https://doi.org/10.1175/2011jcli4003.1

Lind, S., Ingvaldsen, R. B., & Furevik, T. (2018). Arctic warming hotspot in the northern Barents Sea linked to declining sea-ice import. *Nature Climate Change*, *8*(7), 634–639. https://doi.org/10.1038/s41558-018-0205-y

Luo, D., Yao, Y., & Dai, A. (2015). Decadal relationship between European blocking and the North Atlantic Oscillation during 1978–2011. Part I: Atlantic conditions. *Journal of the Atmospheric Sciences*, *72*(3), 1152–1173. https://doi.org/10.1175/jas-d-14-0039.1

Luo, D. H., Xiao, Y., Yao, Y., Dai, A., Simmonds, I., & Franzke, C. L. E. (2016). Impact of Ural blocking on winter warm Arctic-cold Eurasian anomalies. Part I: Blocking-induced amplification. *Journal of Climate*, *29*(11), 3925–3947. https://doi.org/10.1175/Jcli-D-15-0611.1

Matsumura, S., & Kosaka, Y. (2019). Arctic-Eurasian climate linkage induced by tropical ocean variability. *Nature Communications*, *10*(1), 3441. https://doi.org/10.1038/s41467-019-11359-7

McCusker, K. E., Fyfe, J. C., & Sigmond, M. (2016). Twenty-five winters of unexpected Eurasian cooling unlikely due to Arctic sea-ice loss. *Nature Geoscience*, *9*(11), 838–884. https://doi.org/10.1038/ngeo2820

Meleshko, V. P., Johannessen, O. M., Baidin, A. V., Pavlova, T. V., & Govorkova, V. A. (2016). Arctic amplification: Does it impact the polar jet stream? *Tellus*, *68*(1), 32330. https://doi.org/10.3402/tellusa.v68.3233

Nakamura, T., Yamazaki, K., Iwamoto, K., Honda, M., Miyoshi, Y., Ogawa, Y., & Ukita, J. (2015). A negative phase shift of the winter AO/NAO due to the recent Arctic sea-ice reduction in late autumn. *Journal of Geophysical Research: Atmospheres*, *120*, 3209–3227. https://doi.org/10.1002/2014JD022848

Nakamura, T., Yamazaki, K., Sato, T., & Ukita, J. (2019). Memory effects of Eurasian land processes cause enhanced cooling in response to sea ice loss. *Nature Communications*, *10*(1), 5111. https://doi.org/10.1038/s41467-019-13124-2

Ogawa, F., Keenlyside, N., Gao, Y., Koenigk, T., Yang, S., Suo, L., et al. (2018). Evaluating impacts of recent Arctic sea ice loss on the northern hemisphere winter climate change. *Geophysical Research Letters*, *45*, 3255–3263. https://doi.org/10.1002/2017GL076502

Overland, J. E., & Wang, M. (2010). Large-scale atmospheric circulation changes are associated with the recent loss of Arctic sea ice. *Tellus A*, *62*(1), 1–9.

Peings, Y. (2019). Ural blocking as a driver of early-winter stratospheric warmings. *Geophysical Research Letters*, *46*, 5460–5468. https://doi.org/10.1029/2019GL082097

Peings, Y., & Magnusdottir, G. (2014). Forcing of the wintertime atmospheric circulation by the multidecadal fluctuations of the North Atlantic Ocean. *Environmental Research Letters*, *9*, 034018.

Screen, J. A. (2017). The missing Northern European winter cooling response to Arctic sea ice loss. *Nature Communications*, *8*, 14,603.

Screen, J. A., Deser, C., & Simmonds, I. (2012). Local and remote controls on observed Arctic warming. *Geophysical Research Letters*, *39*, L10709. https://doi.org/10.1029/2012GL051598

Screen, J. A., & Simmonds, I. (2010). The central role of diminishing sea ice in recent Arctic temperature amplification. *Nature*, *464*(7293), 1334–1337. https://doi.org/10.1038/nature09051

Sellevold, R., Sobolowski, S., & Li, C. (2016). Investigating possible Arctic-midlatitude teleconnections in a linear framework. *Journal of Climate*, *29*(20), 7329–7343. https://doi.org/10.1175/Jcli-D-15-0902.1

Stroeve, J., & Notz, D. (2018). Changing state of Arctic sea ice across all seasons. *Environmental Research Letters*, *13*(10), 103,001. https://doi.org/10.1088/1748-9326/aade56

Takaya, K., & Nakamura, H. (2001). A formulation of a phase-independent wave-activity flux for stationary and migratory quasigeostrophic eddies on a zonally varying basic flow. *Journal of the Atmospheric Sciences*, *58*(6), 608–627. https://doi.org/10.1175/1520-0469(2001)058<0608:afoapi>2.0.co;2

Tyrlis, E., Manzini, E., Bader, J., Ukita, J., Nakamura, H., & Matei, D. (2019). Ural blocking driving extreme Arctic sea ice loss, cold Eurasia, and stratospheric vortex weakening in autumn and early winter 2016–2017. *Journal of Geophysical Research: Atmospheres*, *124*, 11,313–11,329. https://doi.org/10.1029/2019JD031085

Vavrus, S. J. (2018). The influence of Arctic amplification on mid-latitude weather and climate. *Current Climate Change Reports*, *4*(3), 238–249.

Warner, J. L., Screen, J. A., & Scaife, A. A. (2020). Links between Barents-Kara sea ice and the extratropical atmospheric circulation explained by internal variability and tropical forcing. *Geophysical Research Letters*, *47*, e2019GL085679. https://doi.org/10.1029/2019GL085679

Wernli, H., & Papritz, L. (2018). Role of polar anticyclones and mid-latitude cyclones for Arctic summertime sea-ice melting. *Nature Geoscience*, *11*(2), 108–113. https://doi.org/10.1038/s41561-017-0041-0

Xu, X., He, S., Gao, Y., Furevik, T., Wang, H., Li, F., & Ogawa, F. (2019). Strengthened linkage between midlatitudes and Arctic in boreal winter. *Climate Dynamics*, *53*(7-8), 3971–3983. https://doi.org/10.1007/s00382-019-04764-7

Ye, K., Jung, T., & Semmler, T. (2018). The influences of the Arctic troposphere on the midlatitude climate variability and the recent Eurasian cooling. *Journal of Geophysical Research: Atmospheres*, *123*, 10,162–10,184. https://doi.org/10.1029/2018JD028980

Zhang, J., Tian, W., Chipperfield, M. P., Xie, F., & Huang, J. (2016). Persistent shift of the Arctic polar vortex towards the Eurasian continent in recent decades. *Nature Climate Change*, *6*(12), 1094–1099. https://doi.org/10.1038/nclimate3136

Zhang, P., Wu, Y., Simpson, I. R., Smith, K. L., Zhang, X., De, B., & Callaghan, P. (2018). A stratospheric pathway linking a colder Siberia to Barents-Kara Sea sea ice loss. *Science Advances*, *4*(7), eaat6025. https://doi.org/10.1126/sciadv.aat6025